The structure and properties of water-based silicone blended phenolic resin and its application in oil filter paper-based materials

Lele Sun, Jin Yang[†], and Jun Yan

Engineering Research Center of Papermaking and Pollution Control, School of Light Industry Science and Engineering,
State Key Lab of Pulp and Paper Engineering, South China University of Technology, Guangzhou, 510641, China

Abstract−The research on water-based and enhanced modification of phenolic resin for impregnation of automobile engine oil filter paper has attracted widespread attention. First, the organosilicon was modified, the polyoxyethylene ether (PEO) and allyl glycidyl ether (AGE) were introduced through the hydrosilylation reaction, and the optimal modification conditions of PEO and AGE were discussed. The results show that when the PEO:AGE molar ratio is 3 : 1, the modified silicone prepared has good dispersibility in water. Scanning electron microscopy (SEM) energy dispersive imaging (EDS) was used to analyze the morphology of resin impregnated filter paper. The results show that when the mass ratio of modified silicone to phenolic resin is 5%, the silicone molecular chains and the phenolic resin form a uniform three-dimensional network structure by bonding through chemical bonds. Compared with unmodified pure phenolic resin impregnated filter paper, the mechanical properties and engine oil resistance properties of the silicone-modified phenolic resin-impregnated filter paper are improved.

Keywords: Blending Modification, Phenolic Resin, Micro Morphology, Organic Silicon, Paper-based Material

INTRODUCTION

The working medium environment of fuel filter paper and oil filter paper of automobile engine filter is gasoline, diesel, and engine oil. It has strong dissolving and corrosive ability and high operating temperature [1-8]. To meet the requirements of environmental protection and safe production, water-based phenolic resin is mainly used to protect filters and enhance the mechanical properties of paper-based materials. However, due to small molecular weight, water-soluble phenolic resins will co-distill between the small phenolic molecules and water molecules during high temperature curing and heat transfer to the surface of the paper through the "wick" of the fiber, thereby reducing the filtration performance of the paper [9-15]. Low molecular weight leads to lower mechanical properties, and the prepared oil filter paper shows brittleness.

In this research, first, water-based silicone was prepared through hydrosilylation [16-22] and further blended with water-based phenolic [23-26]. Finally, silicone and hydrosilylation water-based phenolic formed a stable three-dimensional network structure, which was applied to the reinforcement of oil filter paper-based materials [27,28]. The microscopic composition, morphology, structure and properties of paper-based composites were analyzed, and the evolution law and action mechanism of the blend resin were analyzed at the micro level, so as to reveal the inherent correlation between the resin structure and the mechanical properties of paper [29-33].

[†]To whom correspondence should be addressed.
E-mail: yangjin@scut.edu.cn

EXPERIMENTAL

1. Materials and Equipment
1-1. Experimental Materials

Hydrogen-containing silicone oil (PHMS, hydrogen content 1.0) was purchased from China Bluestar Chenguang Research Institute; Chloroplatinic acid (CPA) and Isopropanol (IPA) were purchased from Macleans Biochemical Technology Co., Ltd. (configuration mass concentration 2%); Toluene was purchased from Shanghai Lingfeng Chemical Reagent Co., Ltd.; Allyl glycidyl ether (AGE) was purchased from Shanghai Aladdin Biochemical Technology Co., Ltd.; Allyl polyoxyethylene ether (PEO, molecular weight 750) was purchased from Jurong Ningwu New Materials Co., Ltd. provides; Water-based phenolic (PF, mass concentration 40%) was provided by Guangzhou Huachuang Chemical New Material Technology Development Co., Ltd.

1-2. Experimental Equipment

Confocal laser microscope Leica TCS-SP5, Leica, Germany; Fluorescence spectrometer LS55, Perkin Elmer, USA; Scanning electron microscope EVO18, Zeiss, Germany; Energy spectrometer X-Max20 electric cooling type, Oxford, UK; Differential scanning calorimetry Instrument Q200, American TA Company; Tensile Strength Tester CE062, Sweden L&W Company; Flexural Stiffness Tester 79-25-00-0002, US TMI Company; Burst Strength Tester CE180, Sweden L&W Company;

2. Experimental Process
2-1. Synthesis of Modified Silicone

The mole ratio of PEO/AGE was controlled in a 250 mL three-port flask equipped with thermometer, condensate tube, agitator and water divider. AGE, PEO and toluene solutions were succes-
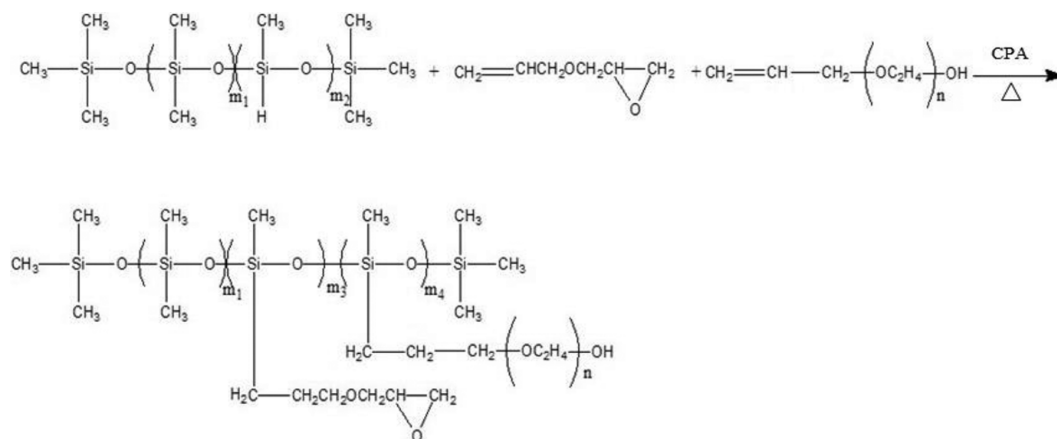
Fig. 1. Reaction equation of modified silicon.

sively added, and isopropyl alcohol chloroplatinate solution was added as catalyst. The temperature was raised to 65 °C under agitation, and quantitative PHMS was slowly added. The temperature was kept at 65 °C for 0.5 h and then raised to 85 °C for 4 h. The solvent was removed by vacuum to obtain a light-colored transparent viscous liquid, denoted as PEO/AGE-g-PHMS. Fig. 1 showed the synthesis formulations of modified silicone.

2-2. Preparation of Silicone Modified Phenolic Resin

The silicone modified phenolic resin was prepared by mixing PEO/AGE-g-PHMS and PF solution in a certain mass ratio, drying and dehydration at 80 °C and curing at 160 °C for 15 min, denoted as (PEO/AGE-g-PHMS)/PF.

2-3. Preparation of Oil Filter Paper

(PEO/AGE-g-PHMS)/PF was dispersed into a 3% water dispersion with deionized water, the base paper was impregnated for 3 minutes and then taken out, controlling the resin sizing amount to (20±0.5)% (Relative to the base paper mass).Then the paper was dried in an oven at 80 °C, and cured at 160 °C for 15 min after the moisture was removed.

TESTING AND CHARACTERIZATION

1. Conversion Rate Test

The hydrogen content of organosilicon was determined by chemical titration method: 0.2 g of the sample was accurately weighed and dissolved in 20 ml of carbon tetrachloride, then 10 ml of liquid Br_2 acetic acid solution was added, and kept standing away from light for 60 minutes; 25 ml of 10% potassium iodide aqueous solution and a small amount of the starch indicator were added, and 0.1 mol/L $Na_2S_2O_3$ standard solution was used to titrate. The titration ended when the color of the liquid changed from blue to colorless; the consumption of $Na_2S_2O_3$ standard solution (ml) was recorded. The hydrogen content was calculated as follows:

$$H\% = \frac{C(V_1 - V_2) \times 0.05 \times 1.0008}{m} \times 100\%$$

where, C is the molar volume concentration (mol/L); V_1 is the blank sample consumption Volume of standard solution (mL); V_2 is the volume of sodium thiosulfate standard solution consumed by the product sample (mL); m is the graft-modified silicone resin mass (g).

2. Fourier Transform Infrared (FT-IR) Spectroscopy Analysis of Modified Silicone

FT-IR characterization adopts KBr coating method to prepare samples, and the test range is 400-4,000 cm^{-1}.

3. NMR Analysis of Modified Organosilicon

^{1}H-NMR characterization was performed using tetramethylsilane (TMS) as the internal standard and the solvent $CDCl_3$.

4. Characterization of PEO/AGE-g-PHMS Water Dispersibility

The graft-modified silicones with different side chain content and proportions were prepared with water dispersions at a mass ratio of 20%, fully stirred and allowed to stand at room temperature for different periods of time. We observed the state of the water dispersions to determine the dispersion performance of the modified silicone in water.

5. (PEO/AGE-g-PHMS)/PF Compatibility Characterization

PEO/AGE-g-PHMS and PF blends with 5%, 10% and 15% absolute dry mass ratio were mixed into 20% aqueous dispersion to observe the blending state.

6. DSC Characterization

The temperature control range of DSC differential scanning calorimetry analysis was room temperature −300 °C, nitrogen atmosphere protection, condition 10 °C/min.

7. Fluorescence Performance Characterization

LS55 fluorescence spectrometer (Perkin Elmer, USA) was used to obtain the fluorescence excitation spectra of PEO/AGE-g-PHMS, PF and (PEO/AGE-g-PHMS)/PF at different excitation wavelengths.

8. Characterization of Confocal Laser Microscopy

A Leica TCS-SP5 confocal laser microscope was used to perform single-photon imaging characterization of (PEO/AGE-g-PHMS)/PF before and after curing, the laser intensity was 20%, the 40X oil lens was used, and the immersion liquid was Type F.

9. SEM-EDS Characterization

EVO18 scanning electron microscope (Leica, Germany) with X-Max20 electric refrigeration spectrometer (Oxford, UK) was used to perform microscopic characterization and energy spectrum imaging of (PEO/AGE-g-PHMS)/PF and oil filter paper. The acceleration voltage of the emission scanning electron microscope was
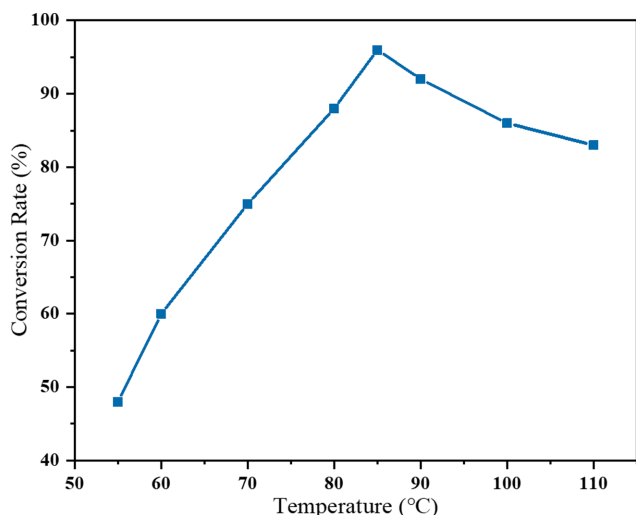
Fig. 2. Effect of reaction temperature on conversion.

adjusted to 20 kv.

We used EVO18's built-in energy spectrum imaging function for characterization, removed the influence of other unnecessary elements, only keeping C, O, and Si, respectively, making the distribution map of the three elements and the image superimposed with the bright field.

10. Characterization of Mechanical Properties of Oil Filter Paper

The impregnated filter paper was placed under 23 °C, 50% RH for 24 h to test its mechanical properties.

11. Characterization of Oil Resistance of Impregnated Filter Paper

The oil resistance properties of the oil filter paper were evaluated by the following method (TB/T3056.2-2002): the impregnated filter paper was first immersed into engine oil at 160 °C for 48 h, and the oil stains on the surface were wiped and the bending stiffness, burst strength and tensile strength were tested.

RESULTS AND DISCUSSION

1. Influence of Reaction Temperature and Time on Conversion Rate

Under the condition of catalyst dosage of 30 μg/g and reaction time of 4 h, the effect of reaction temperature on the conversion was analyzed. It can be seen from Fig. 2 that the conversion rate increases with the increase of temperature below 85 °C, and when the temperature is higher than 85 °C, the conversion rate decreases

Table 1. Effect of reaction time on conversion

Time/h	2	3	4	5	6	8
Conversion rate/%	55.5	72.6	96.3	Gel	Gel	Gel

with the increase of temperature. This is because the Si-H bond has higher bond energy, the Si-H bond can be broken and the catalyst can be activated better under the condition of temperature rise. When the reaction temperature is too high, a series of side reactions will happen, such as dehydrogenation crosslinking reaction of hydrogen-containing silicone oil, and thermal polymerization of unsaturated double bonds contained in AGE and PEO, reducing its conversion rate.

Under the conditions of catalyst dosage 30 μg/g and reaction temperature 85 °C, the effect of reaction time on the conversion rate was analyzed. It can be seen from Table 1 that when the reaction time is 4 h, the conversion rate is the highest, reaching 96.3%. When the reaction time is longer than 5 h, the reactants will gelate and the desired products cannot be obtained. This is because the hydrogen-containing silicone oil undergoes self-dehydrogenation and cross-linking reaction, and the unsaturated double bonds contained in AGE and PEO undergo thermal polymerization, epoxy group ring-opening reaction and a series of side reactions, causing the conversion rate to decrease.

Overall consideration: when the reaction temperature of AGE and PEO co-graft modified silicone is 85 °C and the reaction time is 4 h, the silicon-hydrogen conversion is the highest, reaching 96.3%.

2. Water Dispersibility of PEO/AGE-g-PHMS

In the graft modified silicone, the addition of PEO can make the silicone material water-soluble and disperse stably in water, which is conducive to a physical compound with water-soluble phenolic resin. The addition of AGE is to introduce epoxy groups with high reactivity into the silicone, so that it can be chemically copolymerized with phenolic resin under certain conditions. Therefore, the ratio of PEO/AGE should be moderate, so that it has appropriate reaction functional groups on the premise of ensuring water solubility.
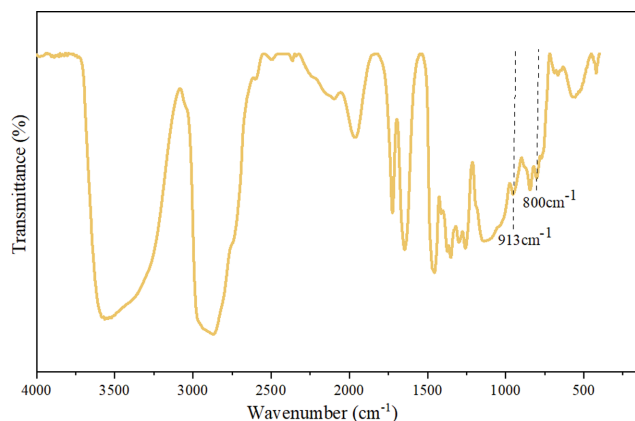
It can be seen from Table 2 that with the increase of PEO content, the side-chain silicone presents a "precipitation-emulsion-transparency" trend in water. When the ratio of PEO/AGE is greater than 3 : 1, the modified organosilicon can be stably dispersed in water, and it still remains colorless and transparent after a long time of standing, indicating that the synthesized product has good stability in water. Considered comprehensively, the side chain silicone prepared with PEO : AGE=3 : 1 (molar ratio) was selected to give the silicone hydrophilicity and at the same time possess a suitable

Table 2. Water dispersibility of modified silicone

PEO/AGE (molar ratio)		1 : 1	2 : 1	2.5 : 1	3 : 1	4 : 1
0 h	Standing	Precipitation	Emulsion	Emulsion	Transparent	Transparent
	Centrifugal	Precipitation	Precipitation	Emulsion	Transparent	Transparent
12 h	Standing	Precipitation	Stratification	Stratification	Transparent	Transparent
	Centrifugal	Precipitation	Precipitation	Emulsion	Transparent	Transparent
72 h	Standing	Precipitation	Stratification	Stratification	Transparent	Transparent
	Centrifugal	Precipitation	Precipitation	Emulsion	Transparent	Transparent

Table 3. Compatibility of (PEO/AGE-g-PHMS)/PF

(PEO/AGE-g-PHMS)/PF (Mass ratio)	5%	10%	15%
0 h	Transparent	Transparent	Turbid liquid
12 h	Transparent	Transparent	Precipitation
48 h	Transparent	Little Precipitation	Precipitation

Fig. 3. FT-IR spectrum of PEO/AGE-g-PHMS.

Fig. 4. NMR spectrum of PEO/AGE-g-PHMS.

amount of reactive epoxy groups.
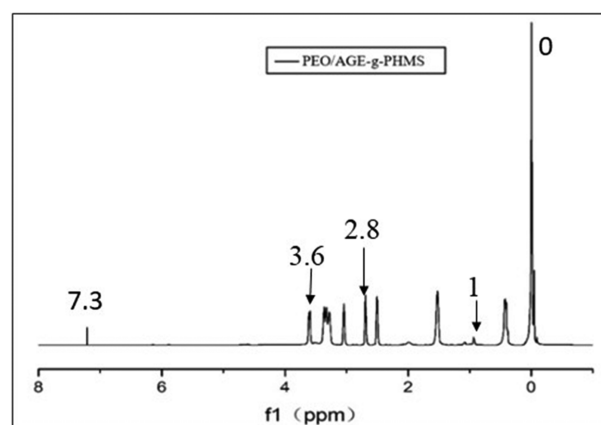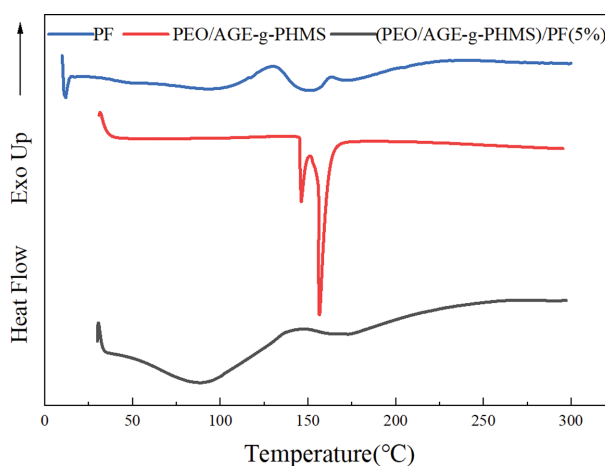
3. Compatibility of (PEO/AGE-g-PHMS)/PF

With the increase of PEO/AGE-g-PHMS, the blended solution showed a process from transparent to turbid liquid and finally formed precipitation. The results are shown in Table 3. This is because the introduction of hydrophilic groups on the side chain of PEO/AGE-g-PHMS forms a strong hydrogen bond with water molecules, which destroys the association between the methylol of water-based PF and water molecules, and reduces the dilution ratio (water number) of phenolic resin, causing the phenolic resin to precipitate. On the other hand, the epoxy group of PEO/AGE-g-PHMS may undergo a ring-opening reaction under alkaline conditions and copolymerize with the phenolic hydroxyl group and methylol group of PF to form cross-linked insolubles.

4. FT-IR Analysis

It can be seen from Fig. 3 that the characteristic absorption of the alcohol hydroxyl group at the end of the grafted polyether is near $3,500\ cm^{-1}$, and the characteristic peak of -CH$_3$, -CH$_2$ appears near $2,900\ cm^{-1}$. The characteristic peak of Si-CH$_3$ is near $800\ cm^{-1}$, while there is no Si-H bond absorption peak near $2,150\ cm^{-1}$. Moreover, the out-of-plane bending vibration peaks of the single substituted double bond at $883\ cm^{-1}$ and $998\ cm^{-1}$ in Fig. 3 disappeared, which can prove that the Si-H bond has reacted with C=C. The characteristic absorption peak of epoxy group appears near $913\ cm^{-1}$, which can be judged that the epoxy group is stable in the process of hydrosilylation. In summary, the disappearance of the Si-H bond and C=C bond indicates that PEO and AGE have been successfully grafted onto the organosilicon molecular chain through the hydrosilylation reaction.

5. NMR Analysis

It can be seen from Fig. 4 that there is no hydrogen proton absorption peak of Si-H near δ=4.65. The proton peaks near δ=0,

Fig. 5. DSC spectra of PF, PEO/AGE-g-PHMS and (PEO/AGE-g-PHMS)/PF(5%).

δ=3.6 represent Si-CH$_3$, and -OC$_2$H$_4$- in polyether, respectively. In the vicinity of δ=2.3-3.5, the chemical shift of hydrogen proton peaks of methylene -CH and methylene -CH$_2$ on the epoxy group is observed The peak at δ=7.3 is that of CDC1$_3$ solvent. It can be seen from the NMR graph that the product produced by the reaction has the expected structure, and both the polyoxyethylene and the epoxy structure are successfully grafted onto the silicone backbone.

6. DSC Analysis

It can be seen from Fig. 5 that the phenolic resin has two exothermic peaks at 130 °C and 160 °C, which corresponds to the curing exotherm of the phenolic resin. First, the methylol groups undergo dehydration and condensation to form ether bonds-CH$_2$-

O-CH$_2$- and then at higher temperature is the process of generating methylene-CH$_2$-.

PEO/AGE-g-PHMS has endothermic peaks at 145 °C and 155 °C, corresponding to the crystalline melting behavior, indicating that the modified silicone has two ordered crystalline structures and the ring-opening exothermic reaction of epoxy groups does not occur during the entire heating process, which shows that the epoxy groups in the modified silicone oil prepared are stable at normal temperature and high temperature.

When the mass ratio of PEO/AGE-g-PHMS in (PEO/AGE-g-PHMS)/PF is 5%, an endothermic process occurs at about 90 °C, corresponding to the removal of physically bound water, which corresponds to the removal of physically bound water. The exothermic peak that begins to appear near 150 °C is a broad peak which is the curing peak of phenolic resin and possible ring-opening copolymerization with epoxy groups. A gentle and continuous endothermic peak appears at about 175 °C which corresponds to the crystalline melting behavior of organosilicon. During the blending process, the deep entanglement between the phenolic resin and the silicone molecular chain causes the phenolic resin amorphous structure to dilute the silicone crystalline area, destroys or weakens the orderly stacking of the silicone molecular chain and makes the original two crystalline structures of modified organic silicon rearranged in the three-dimensional network of the phenolic resin and transforms into an ordered structure distributed in the phenolic resin, forming a stable structure similar to a semi-interpenetrating network.

7. (PEO/AGE-g-PHMS)/PF Single Photon Imaging

The reason for the fluorescence of PEO/AGE-g-PHMS is "aggregation induced luminescence" (AIE). Under the excitation wavelength of 405 nm, PEO/AGE-g-PHMS has a large and broad peak in the range of 820-850 nm, which corresponds to the epoxy group of the side chain of polysiloxane that can emit blue light visible to the naked eye at this wavelength and it has a strong fluorescence
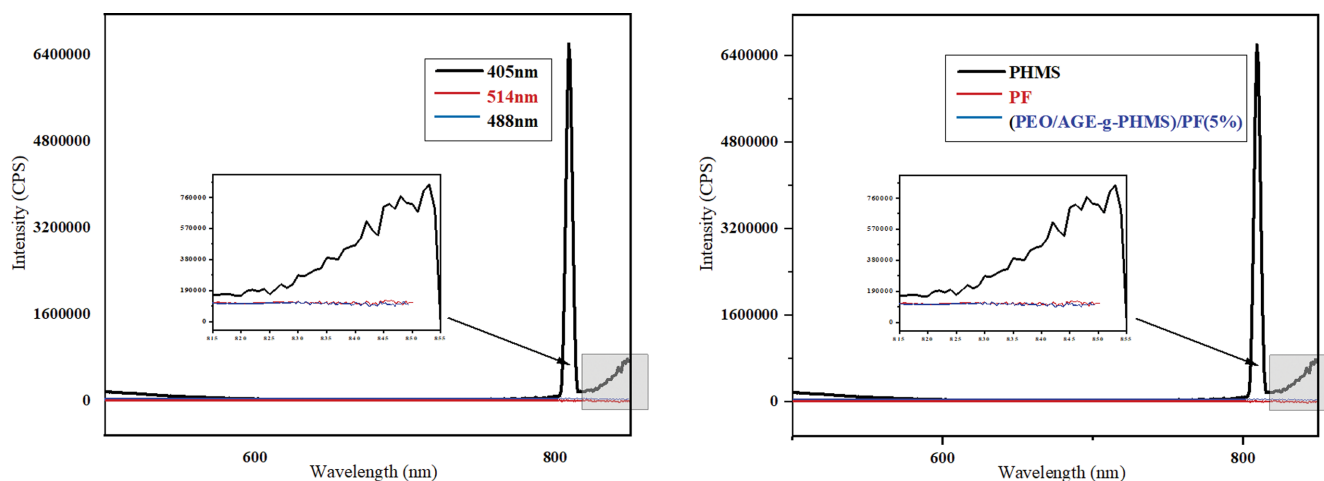

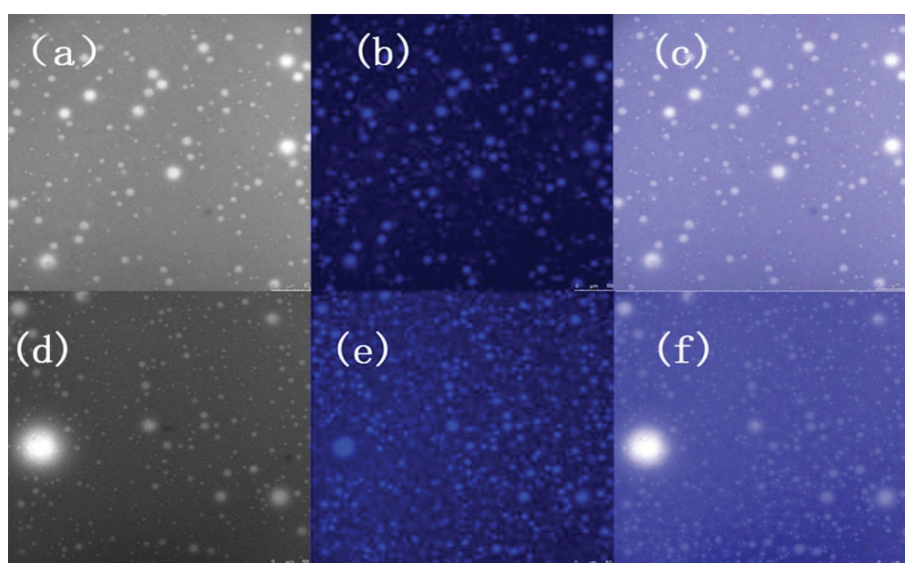Fig. 6. Fluorescence emission spectra of PEO/AGE-g-PHMS, PF and (PEO/AGE-g-PHMS)/PF.

Fig. 7. (PEO/AGE-g-PHMS)/PF (before curing) single photon imaging. (PEO/AGE-g-PHMS)/PF (5%): (a)-bright field (b)-fluorescence field (c)-superimposed field. (PEO/AGE-g-PHMS)/PF (10%): (d)-bright field (e)-fluorescence field (f)-superimposed field.

effect. The fluorescence intensity of PF at this excitation wavelength is almost negligible. At the same time, after the blend of the two is cured at high temperature, if the epoxy group is opened for ring-opening reaction, the fluorescence emission spectrum is similar to PF, and no fluorescence peak is generated. The PEO/AGE-g-PHMS with epoxy group can be easily distinguished by the fluorescence emission spectrum. Therefore, during the formation of blends, single-photon imaging technology is used to track the epoxy group ring-opening reaction process, revealing the evolution process and

law of the blend from the microscopic level.

PEO/AGE-g-PHMS was added with 5% and 10% to form a physical blend with PF and its/the blend single-photon imaging is shown in Fig. 6. There will be white light spots in the bright field, corresponding to blue fluorescence in the fluorescent field and the corresponding substance is PEO/AGE-g-PHMS, indicating that the blend has not undergone epoxy ring opening reaction before heating and curing. PEO/AGE-g-PHMS is dispersed in the PF aqueous solution in the form of small droplets, so the distribution of modi-
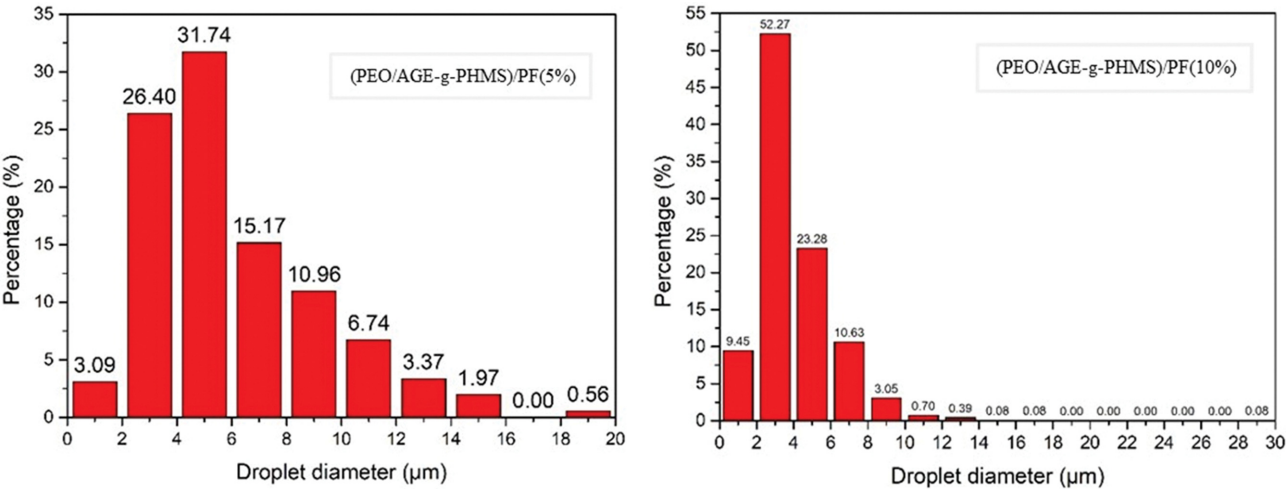

Fig. 8. Diameter distribution of (PEO/AGE-g-PHMS)/PF droplets.

Table 4. Diameter distribution of (PEO/AGE-g-PHMS)/PF droplets

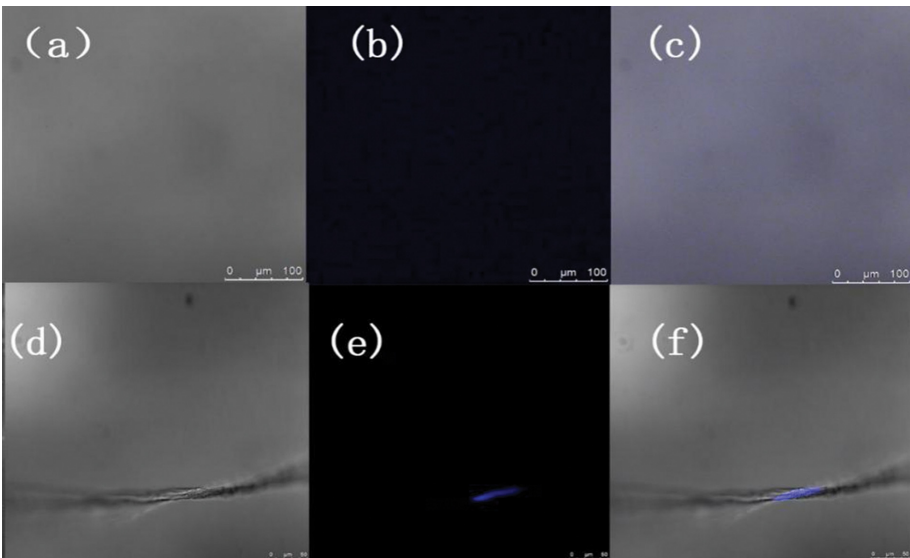| Sample	Statistics	Minimum diameter (μm)	Maximum diameter (μm)	Average diameter (μm)	Dispersion coefficient
(PEO/AGE-g-PHMS)/PF(5%)	356	0.96	18.91	6.03	486.31
(PEO/AGE-g-PHMS)/PF(10%)	1,280	0.99	29.78	3.97	680.03

Fig. 9. (PEO/AGE-g-PHMS)/PF (after curing) single photon imaging. (PEO/AGE-g-PHMS)/PF (5%): (a)-bright field (b)-fluorescence field (c)-superimposed field. (PEO/AGE-g-PHMS)/PF (10%): (d)-bright field (e)-fluorescence field (f)-superimposed field.
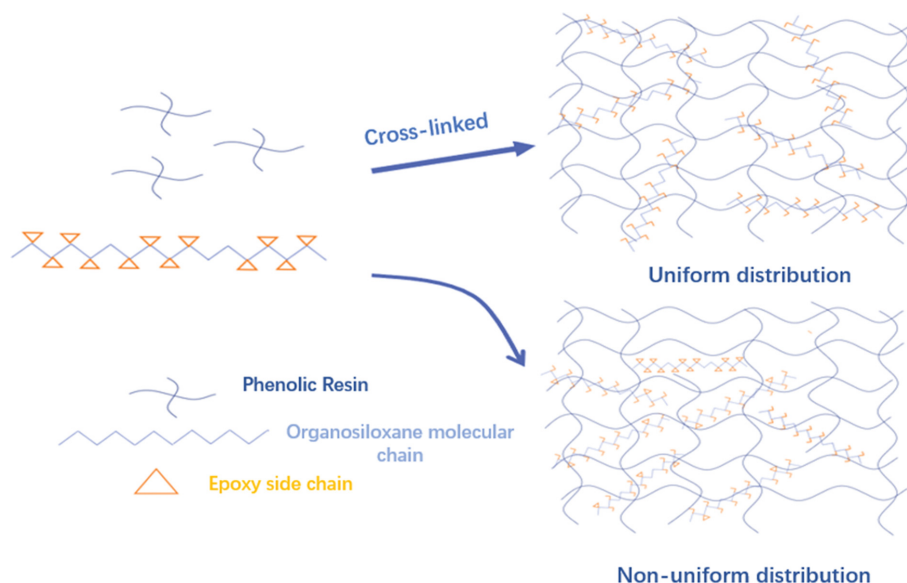
Fig. 10. Schematic diagram of the compounding mechanism of (PEO/AGE-g-PHMS)/PF.

fied silicone in the phenolic resin can be judged by the amount and form of fluorescence.

Comparing Fig. 7(b) and 4(e), with the addition of PEO/AGE-g-PHMS from 5% to 10%, the blue fluorescence increases and the fluorescence intensity also increases. We used Nano Measurer software to mark the droplet diameters in Fig. 7(b) and 4(e). The diameter distribution and statistical data are shown in Fig. 8 and Table 4. When the modified silicone was added at 5%, the modified silicone was uniformly distributed in the blend with droplets with an average diameter of 6.03 μm, most of them concentrated in 4-6 μm, accounting for 31.74%; As the modified silicone content increased to 10%, the average droplet diameter decreased to 3.97 μm, mainly concentrated in 2-4 μm, accounting for 52.27%.

With the increase of the content of PEO/AGE-g-PHMS, the maximum diameter of the droplets increased from 18.91 μm to 29.78 μm, indicating that with the increase of the amount of modified silicone added, there is agglomeration in the local area of the blend system, which leads to the deterioration of uniformity and the dispersion coefficient increasing from 486.31 to 680.03.

After high temperature curing treatment, (PEO/AGE-g-PHMS)/PF forms a solid state and its bright field, fluorescent field and superimposed image are shown in Fig. 9. It can be seen from Fig. 9(a) that when the addition amount of PEO/AGE-g-PHMS is 5%, the epoxy group of the side chain undergoes a ring-opening reaction and loses fluorescence and the blend after high temperature curing becomes smooth sheet-like film, so the distribution of the components of the blend cannot be observed by single-photon imaging. When the addition amount of PEO/AGE-g-PHMS is increased to 10%, the fluorescence of PEO/AGE-g-PHMS will be observed in a small part of the area. This is because with the increase of its content, the modified silicone in the blending system will agglomerate in a local area and the distribution uniformity will decrease. In large-sized aggregated PEO/AGE-g-PHMS, only the epoxy groups on the surface and PF undergo a ring-opening reaction, which prevents the epoxy groups inside the aggregate from further react-

ing after forming a cured product. Therefore, a little fluorescence can still be observed after high-temperature curing.

8. Analysis of the Composite Mechanism of Modified Silicone and Phenolic Resin

Using water as the dispersion medium, when PEO/AGE-g-PHMS is mixed with PF at 5%, PEO/AGE-g-PHMS is evenly distributed in PF, the molecular chains of the two are entangled with each other. The molecular chains of organosiloxane, polyoxyethylene ether and PF penetrate each other, and through the ring-opening reaction of epoxy groups they combine with each other in the form of chemical bonds to form a stable and dense three-dimensional network structure and improve the comprehensive performance of the composite material. When the added amount of modified silicone is increased to 10%, the average diameter of PEO/AGE-g-PHMS decreases from 6.03 μm to 3.97 μm, while the dispersion coefficient increases from the original 486.31 to 680.03 and the dispersibility becomes worse, resulting in larger size aggregation. The maximum diameter of the droplet reaches 29.78 μm, causing a small part of the epoxy groups inside the droplet to be unable to undergo ring-opening reaction and be "wrapped" in the three-dimensional network structure of PF, which is not conducive to the formation of a regular three-dimensional network structure of PF. It will exist in the form of "defects" during the curing process, which is not conducive to the improvement of the overall performance of the blend. The compounding mechanism fow chart as follows Fig. 10.

9. SEM-EDS Analysis of Oil Filter Paper

(PEO/AGE-g-PHMS)/PF was used as the reinforced resin of oil filter paper, and the micromorphology of impregnated filter paper was characterized by SEM. After the resin curing, there was no crack and no large-area continuous film formed. A "point connection" was formed at the fiber interlacing point, and there was no blocking hole phenomenon to ensure the filtration performance of oil filter paper. EDS surface scanning analysis scanned the selected sample surface area and different elements are represented in bright-
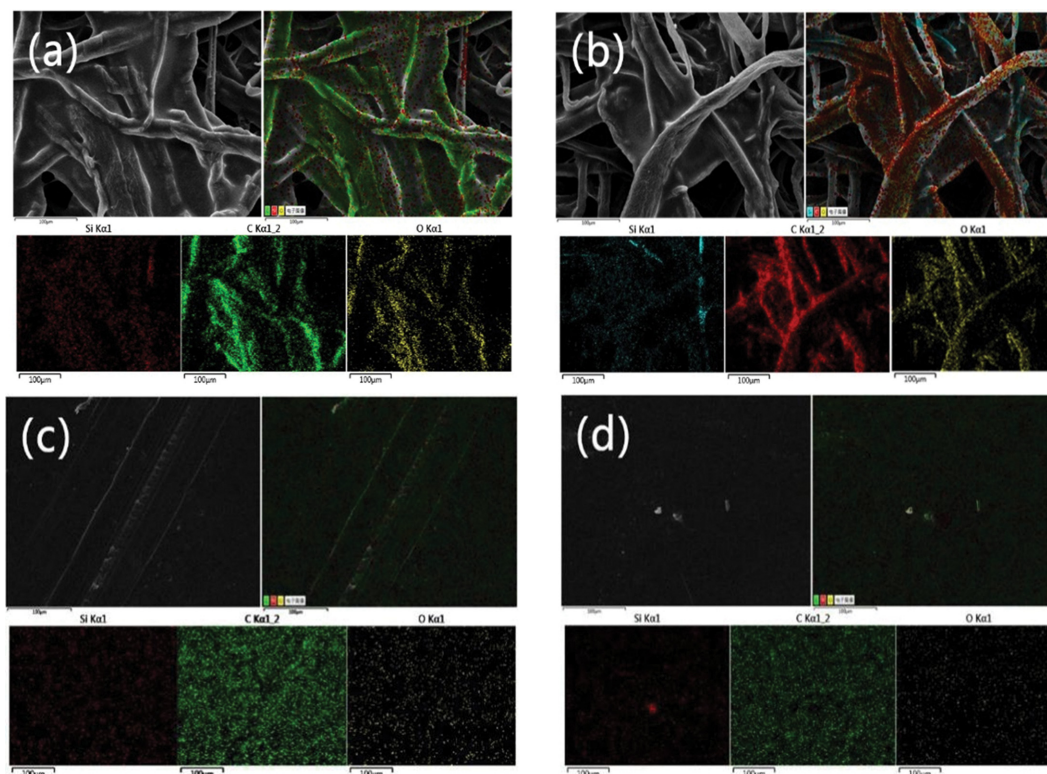
Fig. 11. SEM-EDS analysis of cured resin and its oil filter paper. (a) (PEO/AGE-g-PHMS)/PF (5%) oil filter paper (after curing) SEM-EDS pattern. (b) (PEO/AGE-g-PHMS)/PF (10%) oil filter paper (after curing) SEM-EDS pattern. (c) (PEO/AGE-g-PHMS)/PF (5%) (after curing) SEM-EDS pattern. (d) (PEO/AGE-g-PHMS)/PF (10%) (after curing) SEM-EDS pattern.

ness and color. Combined with scanning electron microscopy morphology analysis, it is often used for qualitative analysis of component agglomeration and element distribution to characterize the element distribution on the plane. Only PEO/AGE-g-PHMS contains Si in the reinforced resin impregnated filter paper, so the distribution of Si can represent the distribution of PEO/AGE-g-PHMS on the paper. It can be seen from Fig. 11(a) that the distribution law of C and O elements is similar, representing the fibers in the paper and corresponding to the fiber bundles in the SEM image. Combined with the SEM image, it can be seen that the surface of the fiber is wrapped by PF, but the Si element is evenly distributed in the PF, indicating that when the addition amount of PEO/AGE-g-PHMS is 5%, the PEO/AGE-g-PHMS is evenly distributed in the PF. The two components are mixed with each other to form a uniform whole, which is attached to the surface and interweaving points of the fibers on the paper.

When the addition of PEO/AGE-g-PHMS increases to 10%, combining the SEM image and the Si element distribution map, it can be seen that Si elements are evenly distributed in PF in most areas. A bright and large area of Si element appears in a very small range, as shown in Fig. 11(b). It shows that PEO/AGE-g-PHMS enrichment occurs in some areas, which is consistent with the analysis of the uneven distribution of size of modified silicone in the blended resin by single-photon imaging technology.

After the blended resin is cured at a high temperature, the ring opening of the epoxy group leads to the disappearance of the single-photon imaging fluorescence and the distribution state of the modified silicone cannot be distinguished. However, the SEM-EDS technology can clearly characterize the distribution of Si element, that is, the distribution of modified silicone in the blend resin. Fig. 11(c) is the EDS diagram of the high temperature curing of the blended resin with 5% modified silicone. The surface of the blended resin is smooth after curing and the C, O, and Si elements are evenly distributed on the surface of the paper fiber; As the amount of modified silicone increases, uneven distribution appears. A bright red spot appears in the central area of Fig. 11(d). The reason is that the epoxy groups on the surface of the large-size modified silicone aggregates are ring-opened and cured, forming a package on the surface, preventing the internal epoxy groups from further reacting with the phenolic resin, thus causing the modified silicone to be enriched in a small part of the area and cannot fully and completely react with the PF.

10. Analysis of Mechanical Properties of Oil Filter Paper

After being toughened by flexible silicone, the activity of the phenolic resin's molecular chain increased. Through hydrogen bonding, physical entanglement and chemical bonding, silicone was "forced to be compatible" with the three-dimensional network structure of phenolic resin, forming a structure similar to "semi-interpenetrating network structure". When the phenolic resin without toughening modification is subjected to external force, stress cracks are generated at the resin/fiber interface due to the stress concentration. The flexible chain structure of organosiloxane and polyoxyethylene ether can be introduced into the cross-linked structure of phenolic resin to increase the activity of its molecular chain and

Table 5. The mechanical properties of oil filter paper

	Bending stiffness /mN	Burst strength /kPa	Tensile strength /kN/m	Elongation /%
Filter paper base paper	70.00	103.00	1.00	1.51
PF	189.10	322.00	5.74	3.36
(PEO/AGE-g-PHMS)/PF (5%)	250.33	414.67	7.35	4.68
(PEO/AGE-g-PHMS)/PF (10%)	244.00	385.33	5.63	3.35

Table 6. Mechanical properties retention rate of impregnated filter paper

Sample	Bending stiffness	Burst strength	Tensile strength
PF	52%	58%	80%
(PEO/AGE-g-PHMS)/PF (5%)	55%	63%	87%

play a role in dispersing stress, thereby enhancing the mechanical properties and toughening the oil filter paper. At the same time, the chemical copolymerization of epoxy groups and phenolic resin also makes the blending system more stable, as the paper fibers are tightly "wrapped and anchored" to improve the mechanical properties of the oil filter paper. Compared with the mechanical properties of pure phenolic impregnated paper, the bending stiffness of the modified sample increased from 189 mN to 250.33 mN, the bursting strength increased from 322 kPa to 414.67 kPa, the tensile strength increased from 5.74 kN/m to 7.35 kN/m and the breaking elongation also increased from 3.36% to 4.68%. The effect of strengthening and toughening was obvious.

It can also be seen from Table 5 that with the increase of modified silicone addition, the mechanical properties of oil filter paper decreased. This is due to the presence of unreacted epoxy groups, similar to "defects" remaining in the blended resin. It is not conducive to the improvement of the performance of the resin and the interface bonding force of the resin/fiber interface, resulting in the degradation of the mechanical properties of the paper. This is consistent with the analysis of the blend structure of the aforementioned resin and the distribution of the resin in the paper sheet.

11. Analysis of Engine Oil Resistance of Impregnated Filter Paper

Because the curable resin tightly "wraps and anchors" the paper fibers, it maintains and protects the structure and performance of the oil filter paper in the oil. Because (PEO/AGE-g-PHMS)/PF (5%) has a three-dimensional network structure of flexible molecular chain and rigid phenolic core bonded by chemical bonds, it can more effectively resist oil damage to paper pages. Therefore, compared with pure phenolic resin impregnated filter paper, the oil resistance properties of phenolic resin impregnated filter paper modified by silicone are improved; it also has a higher retention rate of mechanical properties. The retention rate of stiffness, burst resistance and tensile strength of impregnated filter paper after soaking in engine oil are shown in Table 6.

It can be seen from Table 6 that after being soaked in engine oil at 160 °C, all the mechanical properties have been reduced in different degrees. The retention rates of stiffness, burst resistance and tensile strength of filter paper impregnated with silicone modified phenolic resin are 55%, 63% and 87%, respectively, the retention

rates of all properties are better than that of pure phenolic resin impregnated filter paper. Because of the introduction of silicone material, the link between the phenolic resin molecular chain is strengthened, and the crystallization of silicone ensures that the resin is tightly stacked in the medium of high temperature oil to a certain extent, improving the thermal stability of the blend system, so that the impregnated filter paper can still maintain good mechanical properties after soaking in high temperature oil.

CONCLUSION

By water modification of silicone, a certain proportion of hydrophilic groups and reactive groups were introduced and further blended with water-soluble phenolic resin. When the proportion of modified silicone was 5% and 10%, the blend had good blending stability. The DSC results show that the epoxy groups of the modified silicone were blended with the phenolic resin and then copolymerized with the phenolic resin at high temperature. The original two crystal structures of the modified silicone were rearranged in the three-dimensional network of the phenolic resin. It is transformed into an ordered structure distributed in the phenolic resin, forming a similar semi-interpenetrating network structure, which improves the compatibility of the phenolic resin and silicone.

Single-photon imaging technology was used to analyze the blended resin components and their distribution. The results showed that when the modified silicone resin was added at 5%, droplets with an average diameter of 6.03 μm were uniformly dispersed in the phenolic aqueous solution. However when the content of modified organic silicone reaches 10%, agglomeration and enrichment will occur, the uniformity of the distribution of the components of the blend will be reduced and the silicone agglomerate will become larger. After high-temperature curing, large-size modified silicone can only open epoxy on the surface and combine with phenolic resin to prevent the internal modified silicone from further reacting. It is wrapped in the three-dimensional network system of the resin, which can be distinguished by the fluorescence effect.

Finally, the silicone-modified phenolic resin was used to impregnate and strengthen the automobile filter paper. The micro-element distribution of the oil filter paper was characterized by SEM-

EDS. When the modified silicone was added at 5%, the blended resin was evenly distributed on the surface of the paper fiber and its interlace points. When the added amount reached 10%, enrichment occured in a few areas. Compared with the mechanical properties of pure phenolic impregnated paper, when the added amount of modified silicone was 5%, the strengthening and toughening effect of the paper was obvious, the bending stiffness, burst resistance, tensile strength and elongation were increased by 32%, 21%, 28% and 24% respectively, and the mechanical properties were greatly improved. With the increase of modified silicone addition, the mechanical properties of oil filter paper decreased. This is due to the existence of unreacted epoxy groups, similar to "defects" remaining in the blended resin, which is not conducive to the improvement of the performance of the resin and the bonding force of the resin/fiber interface, resulting in the decrease of mechanical properties of paper. The test results of oil resistance show that the stiffness retention rate, burst resistance retention rate and tensile strength retention rate are 55%, 63% and 87%, respectively, after oil immersion at 160 $^{\circ}$C for 48 h, showing excellent oil resistance.

REFERENCES

1. T. Adachi, T. Kataoka and M. Higuchi, *Int. J. Adhes. Adhes.*, **56**, 53 (2015).
2. Z. J. Xie, C. Liu and G. L. Xu, *J. Vinyl Addit. Technol.*, **27**, 833 (2021).
3. P. Pospiech, J. Chojnowski and U. Mizerska, *J. Mol. Catal. A-Chem.*, **424**, 402 (2016).
4. T. K. Meister, J. W. Kück and K. Riener, *J. Mol. Catal. A-Chem.*, **337**, 157 (2016).
5. A. R. Guo, J. Li and C. Liu, *Chem. J. Chin. Univ.-Chin.*, **37**, 2284 (2016).
6. L. Xu, X. F. Li and Y. M. Zhang, *RSC Adv.*, **11**, 5896 (2021).
7. M. Asima, N. Saba and M. Jawaid, *Curr. Anal. Chem.*, **14**, 185 (2018).
8. J. T. Sunil, A. K. Anoop and R. Joseph, *Int. J. Polym. Mater. Polym. Biomat.*, **59**, 488 (2010).
9. X. J. Yang, S. Liu and Z. Y. Zhao, *Sep. Purif. Technol.*, **255**, 117672 (2021).
10. C. Li, Z. Z. Ma and X. W. Zhang, *Thermochim. Acta*, **639**, 53 (2016).
11. S. Li, F. H. Chen and Y. Han, *Mater. Chem. Phys.*, **165**, 25 (2015).
12. M. Milazzo, A. Amoresano and R. Pasquino, *Macromolecules*, **54**, 11372 (2021).
13. H. Zhang, L. T. Yang and Y. T. Li, *J. Appl. Polym., Sci.*, **17**, 134 (2017).
14. Z. Y. Bu, J. J. Hu and B. G. Li, *Thermochim. Acta*, **575**, 244 (2014).
15. S. Wu, X. Q. Zhang and Y. Sun, *Colloid Polym., Sci.*, **299**, 1327 (2021).
16. J. F. Xi, Y. L. Lou and J. Shan, *Cellulose*, **28**, 10565 (2021).
17. S. H. Siebe, Q. L. Chen and X. Y. Li, *Analyst*, **146**, 1281 (2021).
18. K. Nakamura, J. Nakamura and K. Matsumoto, *J. Taiwan Inst. Chem. Eng.*, **94**, 31 (2019).
19. Y. G. Jiang, Z. P. Zhang and Y. H. Qi, *Polymers*, **13**, 2355 (2021).
20. Q. Q. Zhang, Y. J. Zhu and J. Wu, *J. Colloid Interface Sci.*, **575**, 78 (2020).
21. A. S. Alex, S. Bhuvaneswari and S. C. Chandran, *J. Anal. Appl. Pyrolysis*, **129**, 241 (2018).
22. M. R. Rowles, *J. Appl. Crystallogr.*, **53**, 1625 (2020).
23. B. Sarkar, R. Goyal and C. Pendem, *J. Mol. Catal. A-Chem.*, **424**, 17 (2016).
24. R. J. Han, Y. R. Shao and X. D. Quan, *Polym. Compos.*, **42**, 2370 (2021).
25. C. H. Chen, Y. L. Liou and C. F. Mao, *Polym. Bull.*, **78**, 283 (2021).
26. U. Eduok, O. Faye and J. Szpunar, *Prog. Org. Coat.*, **111**, 124 (2017).
27. X. X. Qin, J. J. Liu and Z. Zhang, *Trac-Trends Anal. Chem.*, **143**, 116371 (2021).
28. S. Piltan, J. Seyfi and I. Hejazi, *Cellulose*, **23**, 3913 (2016).
29. M. Friess, M. Boyukbas and F. Vogel, *Int. J. Appl. Ceram. Technol.*, **19**, 34 (2021).
30. Y. Kotb, A. Cagnard and K. R. Houston, *J. Colloid Interface Sci.*, **608**, 634 (2022).
31. Y. Q. Ling, X. Q. Zhang and L. W. Yan, *Mater. Chem. Phys.*, **275**, 125283 (2022).
32. D. Lin, B. W. Li and J. Qi, *Sens. Actuator B-Chem.*, **303**, 127213 (2020).
33. T. Yin, Q. G. Fu and L. Zhou, *Compos. Pt. B-Eng.*, **192**, 101991 (2020).